Journal of the Korean Magnetic Resonance Society **2000**, *4*, 74-81

NMR Studies on N-terminal Domain of DNA2

Young-Sang Jung, Kyoung-Hwa Lee, Jin-Won Jung and Weontae Lee*

Dept. of Biochemistry, College of Science, Yonsei University, Seoul, 120-740 , Korea
Received July 12, 2000

Abstract: Saccharomyces cerevisiae Dna2 protein has biochemical activities: DNA-dependent ATPase, DNA helicase and DNA nuclease and is essential for cell viability. Especially, Pro^{504} is determined as an important residue in ATPase, helicase, and nuclease activity. We synthesized and determined the three-dimensional solution structure of N-terminal domain comprising residues of Val^{501}-Phe^{508} ($Dna2^{pep}$) using two-dimensional ^{1}H-NMR and dynamical simulated annealing calculations. On the basis of a total of 44 experimental restraints including NOEs, $^3J_{\alpha\beta}$ and $^3J_{\alpha N}$ coupling constants, the solution structures of $Dna2^{pep}$ were calculated with the program CNS. The 23 lowest energy structures were selected out of 50 final simulated-annealing structures. The atomic RMSDs of the final 23 structures for the individual residues were calculated with respect to the average structure. The mean RMSDs for the 23 structures were 0.042 nm for backbone atoms and 0.316 nm for all heavy atoms, respectively. The Ramachandran plot indicates that the ϕ, ψ angles of the 23 final structures are properly distributed in energetically acceptable regions. Solution structure of $Dna2^{pep}$ showed a single unique turn spanning residues of Asn^{503} – Val^{506}.

INTDRODCTION

DNA metabolism is tightly linked to cellular control pathways that regulate the cell division cycle.[1-7] One of the enzymes required to achieve DNA replication, repair, or recombination is the DNA helicase, which uses the energy of ATP to translocate in a specific direction along a DNA strand melting the duplex regions it encounters.[8-12] The single-stranded DNA generated by the helicase is utilized by other enzymes that participate in the subsequent steps in DNA metabolic pathways. Recently, the DNA2 gene of Saccharomyces cerevisiae was implicated in chromosomal DNA replication.[13-14] DNA2 was originally identified by screening for cell division cycle mutants of S. cerevisiae and was shown to be essential for cell viability and to encode a 172 kDa protein with characteristic DNA helicase motifs.[13] A mutation in the C-terminal third of the protein affects helicase and ATPase activity; a mutation in the N-terminal domain (especially at position 504) affects ATPase,

*To whom : wlee@nestis.younsei.ac.kr

helicase, and nuclease. Since the P504S mutation is temperature-sensitive, the mutation may disrupt the conformation of the protein rather than be critical to activities of Dna2 protein. It is therefore necessary to define the structural stability of P504 in Dna2 protein in order to address the issues involved in the native structure of the Dna2 protein. In this report, we present the solution structure of a N-terminal fragment comprising residues of 501 to 508 ($Dna2^{pep}$) to analyze its local conformation using 2D NMR spectroscopy.

MATEREALS AND METHODS

Sample Preparation

The N-terminal peptide of Dna2 comprising residues of Val^{501} to Phe^{508} (Val-Leu-Asn-Pro-Asp-Val-Leu-Phe) was synthesized commercially using solid-phase synthesis (Genosys Biotechnologies, Inc.). Peptides were purified by reverse-phase liquid chromatography using a Vydac VY-DACRP C-8 COLUMN on a Waters Delta Prep 4000 system. Purification was achieved by equilibrating the column with 0.1% trifluoroacetic acid in water and developing with a linear gradient of acetonitrile. All of the purified peptides were finally characterized by combined HPLC and mass spectrometry. The peptide samples for NMR experiments were dissolved in 0.5mL H_2O, at pH 7.2.

NMR Spectroscopy

All ^1H 2D NMR measurements were carried out using a Bruker DRX500 spectrometer in quadrature detection mode equipped with a triple-resonance probe with an actively shielded pulsed-field gradient (PFG) coil. Two-dimensional nuclear Overhauser effect spectroscopy (NOESY) spectra[15] were recorded with mixing times in the range of 400-800 ms. Total correlation spectroscopy (TOCSY) spectrum[16] was acquired in H_2O solution with a mixing time of 78 ms using MLEV17 spin-lock pulses. Double quantum-filtered (DQF) COSY spectra[17] were collected in H_2O to obtain vicinal coupling constant values. All experiments were performed in the phase sensitive mode using the time-proportional-phase-incrementation (TPPI) method[18] with 2048 data points in the t_2 domain and 256 in t_1 domain. Spectra were processed with XWIN-NMR (Bruker instruments) software, running on a Silicon Graphics Indigo^2 workstation. Prior to Fourier transformation in t_1 dimension, the first row was half-weighted to suppress t_1 ridges.[19] The DQF-COSY data were processed to 8192 × 1024 data matrices to get a maximum digital resolution for coupling constant measurements. The proton chemical shifts were referenced with internal sodium 4,4-dimethyl-4-silapentane 1-solfonate.

Molecular modeling calculations

Structure calculations were performed using a hybrid distance geometry and dynamical simulated-annealing protocol with the CNS 1.0 program on a SGI Indigo^2 workstation. The methodology employed by us was similar to the original protocol of Clore

and Gronenborn and their coworkers.[20-22] Distance geometry (DG) substructures were generated using a subset of atoms in the peptide and followed a refinement protocol described in Lee et al.[23]. The target function for molecular dynamics and energy minimization consisted of covalent structure, van der Waals repulsion, NOEs and torsion angle constraints. The torsion angle and NOE constraints were represented by square-well potentials. Based on cross-peak intensities in the NOESY spectra with mixing times of 400, 600, and 800 ms, the distance constraints were classified into three distance ranges, strong (1.8-2.7 Å), medium (1.8-3.3 Å) and weak (1.8-5.0 Å). Pseudoatom corrections were used for non-stereo-specifically assigned methylene protons, methyl groups and the ring protons of phenylalaine residue.[24] The NOESY spectra of Dna2^{pep} yielded 40 NOE constraints. Constraints for the dihedral angles ϕ, χ_1 were deduced on the basis of the $^3J_{HN}$, $^3J_{\alpha\beta}$ coupling constants from 1-D and 2-D DQF-COSY spectra in H_2O solution. All modeling calculation was performed within CNS 1.0 program on a SGI Indigo^2 workstation. The visual analysis of resulting structures was carried out with MOLMOL software[25] running on Silicon Graphics workstations and RMSD values were also obtained from CNS 1.0 software.

RESULT AND DISCUSSION

Resonance Assignments

The proton resonances were identified using the methods proposed by Wuthrich[22]. The first step involved an analysis of the TOCSY and NOESY experiments to identify the spin systems of particular amino acids. It was straightforward enough to assign two valines and leucines because these residues showed characteristic NH chemical shift in the TOCSY spectrum. The spin system identification was completed through an analysis of the TOCSY spectra, and the NOESY spectrum served to identify all sequential connectivities for adjacent residues. The finger print region and amide-amide region of the NOESY spectrum in H_2O solution are shown in Fig. 1. Val^{501}C$^{\alpha}$H/Val^{501}NH, Leu^{502}C$^{\alpha}$H/Leu^{502}HN and Leu^{502}C$^{\alpha}$H/Asp^{503}NH peaks were not found in the NOESY spectrum. It means N-terminal of Dna2^{pep} structure is flexible. Asp505C$^{\beta}$H and Phe508C$^{\beta}$H peaks are assigned stereo specifically with NOESY and DQF-COSY experiment. Fig. 2A. summaries NMR data for the Dna2^{pep} showing sequential and short–range NOE contacts. In Fig. 2B. inter and intra-residue NOE contacts of Dna2^{pep} were displayed based on NOE data. NH/NH NOEs for Asp^{505}-Phe^{508} connectivity shows Dna2^{pep} structure has a rigid turn type.

Distance geometry calculations were employed using constraints obtained from NOESY spectra in water and yielded 50 $<SA>_k$ structures. All of the structures showed no constraint violations greater than 0.03nm for distances and 5° for torsion angles. The 23 lowest energy structures ($<SA>_k$) were selected out of 50 final simulated-annealing structures for further structural analysis. The average structure ($<SA>_k$) was calculated from

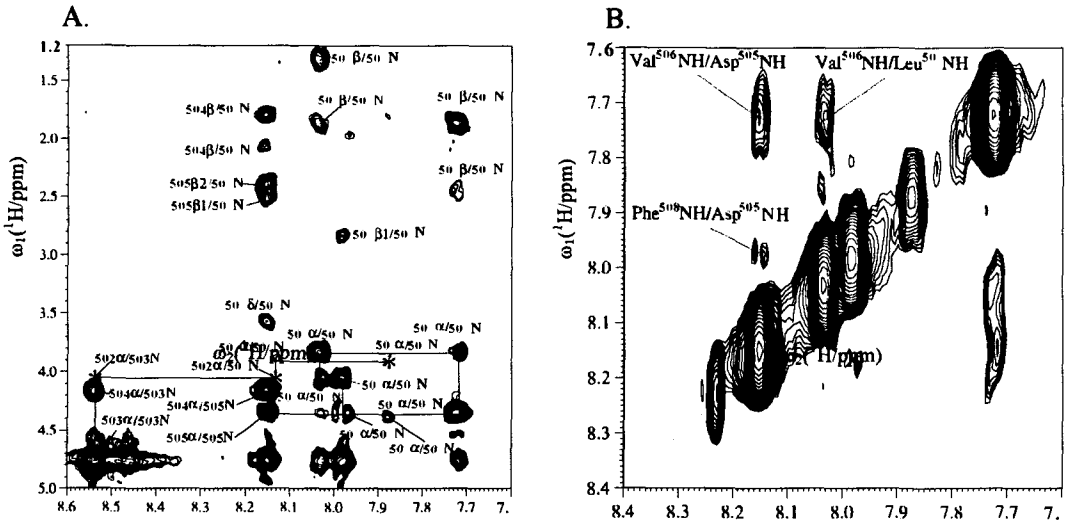

Fig. 1. Two-dimensional ^{1}H NOESY Spectra of Dna2^{pep} in (A) fingerprint and (B) $d_{NN(i,i+1)}$ contact regions at 25°C.

the geometrical average from 23 $<SA>_k$ structure coordinates and subjected to restraint energy minimization (REM) to correct covalent bonds and angle distortions. The energies and structural statistics of the final 23 simulated annealing structures related to experimental constraints were listed in the table 1. The structural statistics associated with the 23 final $<SA>_k$ structures were summarized in the table 2. Ramachandran plots indicate that the , ψ angles of the 23 final structures are properly distributed in energetically acceptable regions. A best-fit superposition of the 23 final NMR structures is displayed in stereo view in Fig. 3. All backbone atoms are superimposed from Asn^{503} form Val^{506} residues.

Structure and Activity Correlation

The 23 structures possess the same overall fold, with a low RMSD value all along the polypeptide chain. Solution structure of nuclease activity domain of Dna2 showed a single unique turn spanning residues of Asn^{503} – Val^{506} containing Pro^{504}. In the Dna2 ts-mutant, this Pro^{504} was replaced Ser residue. This must be the major cause of unstable characters of this mutant protein. From this, it is postulated that Pro^{504} is very important for Dna2 activity. This region may also be involved in domain folding, active site forming or interacting site for other proteins. Together with this structural data, we conclude that the point mutant protein in this region may disturb the biological activity of this motif, perturbing the global structures of Dna2 protein.

A.

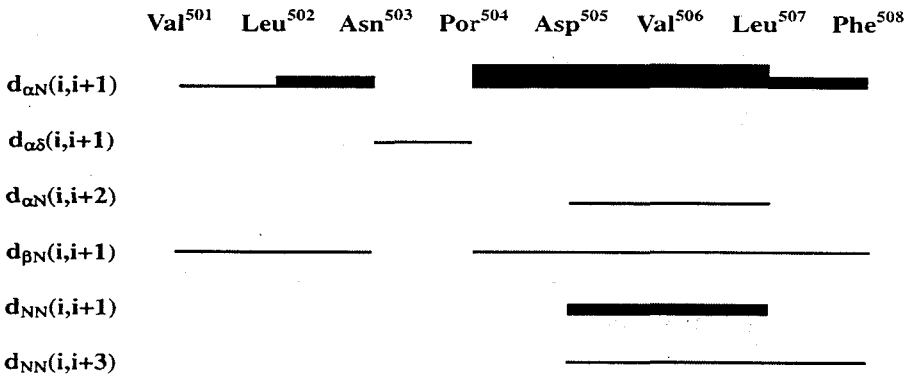

B.

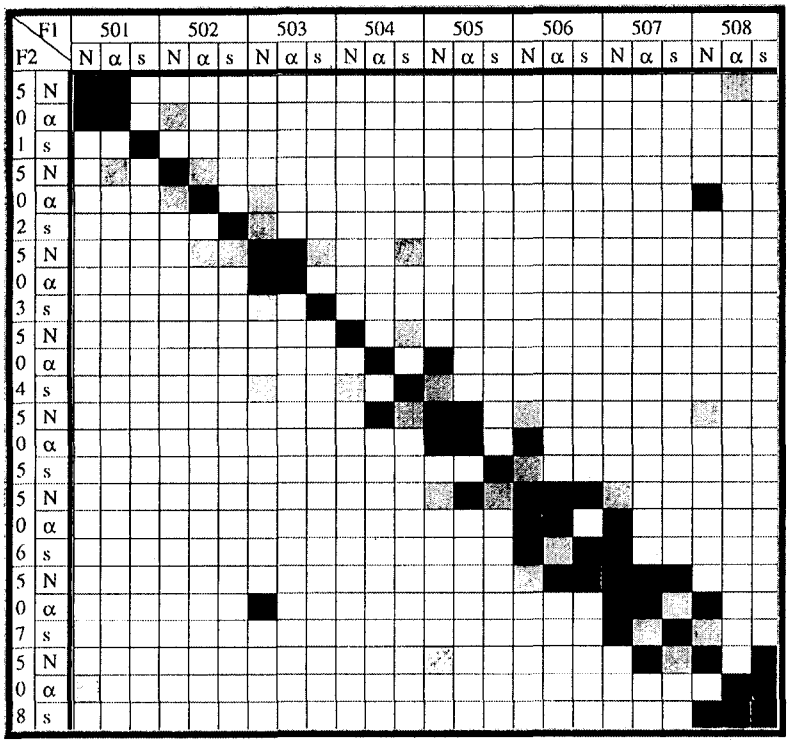

Fig. 2. (A) The sequential and medium-range NOE connectivities of Dna2^{pep} (B) Inter and intra-residue NOE contact-diagram. Amide proton(N), alpha proton(α) and side chain(S) were denoted.

Table 1. Atomic R.M.S.D.s for the 23 Final Simulated Annealing Structures of $Dna2^{pep}$

	$\langle SA \rangle_k$	$\langle SA \rangle_{kr}$
Energy (kcal/mol)		
Total	27.75	23.31
Bonds	1.90	1.55
Angles	14.32	13.29
Improper	0.15	0.12
Van der Waals	4.15	4.03
NOE	7.19	7.90
Lennard-Jones†	-99.5	-81.4
RMSD		
Bonds (Å)	0.0037	0.0034
Angles (deg)	0.6182	0.5957
NOE (Å)	0.0490	0.0628

† Lennard-Jones/van der Waals potential was calculated using the CHARMm empirical energy function.

Table 2. Structural Statistics for the 23 Final Simulated Annealing Structures of $Dna2^{pep}$.

Parameters	Backbone Atoms (Å)	All Atoms (Å)
$\langle SA \rangle_k$ vs. $\langle \overline{SA} \rangle_k$	0.898	2.110
$\overline{\langle SA \rangle_k}$ vs. $\langle \overline{SA} \rangle_k$	0.988	1.835
$\langle SA \rangle_k$ vs. $\overline{\langle SA \rangle_k}$	0.919	2.171

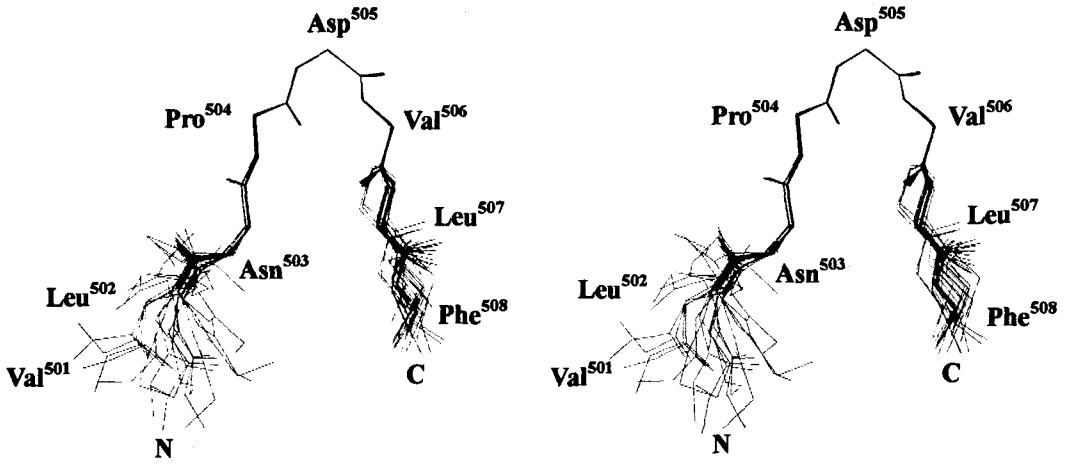

Fig. 3. Stereoview of the backbone superposition of the 23 final simulated annealing structures of $Dna2^{pep}$.

REFERENCE

1. Murray, A., Hunt, T., "*The Cell Cycle: An Introduction*", pp. 135-152, Oxford University Press, New York, 1993.
2. Hartwell, L. H., Kastan, M. B., *Science*, **266**, 1821-1828 (1994).
3. Murray, A. W. Curr. Opin. Genet. & Dev. 5, 5-11 (1995).
4. Elledge, S. J., *Science*, **274**, 1664-1672 (1996).
5. Kaufmann, W. K., Paules, R. S., *FASEB J.*, **10**, 238-247 (1996).
6. Lydall, D., Weinert, T. Curr. Opin. Genet. & Dev. 6, 4-11 (1996).
7. Weinert, T., *Cancer Surv.*, **29**, 109-132 (1997).
8. Matson, S. W., Kaiser-Rogers, K. A., *Annu. Rev. Biochem.*, **59**, 289-329 (1990).
9. Thömmes, P., Hübscher, U., *Chromosoma (Berl.)*, **101**, 467-473 (1992).
10. Lohman, T. M., Bjornson, K. P., *Annu. Rev. Biochem.*, **65**, 169-214 (1996).
11. Tuteja, N., Tuteja, R., *Nat. Genet.*, **13**, 11-12 (1996).
12. West, S. C., *Cell*, **86**, 177-180 (1996).
13. Budd, M. E., Campbell, J. L., *Proc. Natl. Acad. Sci. U. S. A.*, **92**, 7642-7646 (1995).
14. Budd, M. E., Choe, W. C., Campbell, J. L., *J. Biol. Chem.*, **270**, 26766-26769 (1995).
15. Jeener, J., Meier, B.H., Bachman, P., Ernst, R.R., *J. Chem. Phys.*, **71**, 4546-4553 (1979).
16. Davis, D.G., Bax, A. J., *Am. Chem. Soc.*, **107**, 2820-2921 (1985).
17. Rance, M., Sörensen, O.W., Bodenhausen, G., Wagner, G., Ernst, R.R., Wüthrich, K., *Biochem. Biophys. Res. Commun.*, **117**, 479-485 (1983).
18. Marion, D., Wüthrich, K., *Biochem. Biophys. Res. Commun.*, **113**, 967-974, (1983).
19. Otting, G., Widmer, H., Wagner, G., Wüthrich, K., *J. Magn. Reson.*, **66**. 187-193 (1986).

20. Nilges, M., Clore, G.M., Gronenborn, A.M., *FEBS Lett.*, **229**, 317-324 (1988a).
21. Nilges, M., Clore, G.M., Gronenborn, A.M., *FEBS Lett.*, **239**, 129-136 (1988b).